

Predicting Aesthetic Outcome of the Nuss Procedure in Patients with Pectus Excavatum

Citation for published version (APA):

Coorens, N. A., Daemen, J. H. T., Slump, C. H., Janssen, N., Jansen, Y., Maessen, J. G., Vissers, Y. L. J., Hulsewé, K. W. E., & de Loos, E. R. (2023). Predicting Aesthetic Outcome of the Nuss Procedure in Patients with Pectus Excavatum. *Seminars in Thoracic and Cardiovascular Surgery*, 35(3), 627-637. <https://doi.org/10.1053/j.semtcvs.2022.06.007>

Document status and date:

Published: 01/09/2023

DOI:

[10.1053/j.semtcvs.2022.06.007](https://doi.org/10.1053/j.semtcvs.2022.06.007)

Document Version:

Version created as part of publication process; publisher's layout

Document license:

Taverne

Please check the document version of this publication:

- A submitted manuscript is the version of the article upon submission and before peer-review. There can be important differences between the submitted version and the official published version of record. People interested in the research are advised to contact the author for the final version of the publication, or visit the DOI to the publisher's website.
- The final author version and the galley proof are versions of the publication after peer review.
- The final published version features the final layout of the paper including the volume, issue and page numbers.

[Link to publication](#)

General rights

Copyright and moral rights for the publications made accessible in the public portal are retained by the authors and/or other copyright owners and it is a condition of accessing publications that users recognise and abide by the legal requirements associated with these rights.

- Users may download and print one copy of any publication from the public portal for the purpose of private study or research.
- You may not further distribute the material or use it for any profit-making activity or commercial gain
- You may freely distribute the URL identifying the publication in the public portal.

If the publication is distributed under the terms of Article 25fa of the Dutch Copyright Act, indicated by the "Taverne" license above, please follow below link for the End User Agreement:

www.umlib.nl/taverne-license

Take down policy

If you believe that this document breaches copyright please contact us at:

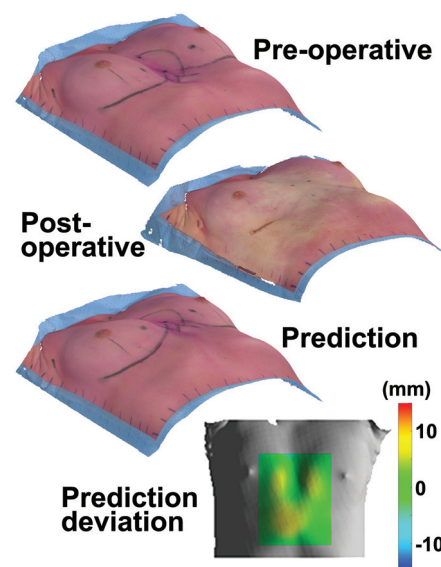
repository@maastrichtuniversity.nl

providing details and we will investigate your claim.

Predicting Aesthetic Outcome of the Nuss Procedure in Patients with Pectus Excavatum

Nadine A. Coorens, MSc,^{*,†} Jean H.T. Daemen, MD,^{*} Cornelis H. Slump, MSc, PhD,[†] Nicky Janssen, MD,^{*} Yanina Jansen, MD, PhD,^{*} Jos G. Maessen, MD, PhD,^{‡,§} Yvonne L.J. Vissers, MD, PhD,^{*} Karel W.E. Hulswé, MD, PhD,^{*} and Erik R. de Loos, MD, PhD^{*}

Patients suffering from pectus excavatum often experience psychosocial distress due to perceived anomalies in their physical appearance. The ability to visually inform patients about their expected aesthetic outcome after surgical correction is still lacking. This study aims to develop an automatic, patient-specific model to predict aesthetic outcome after the Nuss procedure. Patients prospectively received preoperative and postoperative 3-dimensional optical surface scanning of their chest during the Nuss procedure. A prediction model was composed based on nonlinear least squares data-fitting, regression methods and a 2-dimensional Gaussian function with adjustable amplitude, variance, rotation, skewness, and kurtosis components. Morphological features of pectus excavatum were extracted from preoperative images using a previously developed surface analysis tool to generate a patient-specific model. Prediction accuracy was evaluated through cross-validation, utilizing the mean root squared deviation and maximum positive and negative deviations as performance measures. The prediction model was evaluated on 30 (90% male) prospectively imaged patients. The model achieved an average root mean squared deviation of 6.3 ± 2.0 mm, with average maximum positive and negative deviations of 12.7 ± 6.1 and -10.2 ± 5.7 mm, respectively, between the predicted and actual postoperative aesthetic result. Our developed 2-dimensional Gaussian model based on 3-dimensional optical surface images is a clinically promising tool to predict postsurgical aesthetic outcome in patients with pectus excavatum. Prediction of the aesthetic outcome after the Nuss procedure potentially improves information provision and expectation management among patients. Further research should assess whether increasing the sample size may reduce deviations and improve performance.



Prediction of post-operative aesthetic outcome in patients with pectus excavatum.

Central Message

A model based on Gaussian functions and 3-dimensional optical scans is a clinically promising noninvasive tool to predict postsurgical aesthetic outcome in patients with pectus excavatum.

Semin Thoracic Surg ■■■■■-■■■ © 2022 Elsevier Inc. All rights reserved.

Abbreviations: 2D, 2-dimensional; 3D, 3-dimensional; IQR, interquartile range; SD, standard deviation

^{*}Department of Surgery, Division of General Thoracic Surgery, Zuyderland Medical Center, Heerlen, The Netherlands

[†]Faculty of Science and Technology (S&T), University of Twente, Enschede, The Netherlands

[‡]Department of Cardiothoracic Surgery, Maastricht University Medical Center, Maastricht, The Netherlands

[§]Faculty of Health, Medicine and Life Sciences (FHML), Cardiovascular Research Institute Maastricht (CARIM), Maastricht, The Netherlands

Financial Disclosure: This work was supported by the Zuyderland Research and Innovation Fund of Zuyderland Medical Center (Heerlen, the Netherlands) (grant number 2019-005).

Conflicts of Interest: None of the authors had any conflicts to declare.

Institutional Review Board (IRB) Approval: The study was approved by the local research and ethics committee (METCZ; ID: 20200071; approval date: April 14th, 2020).

Informed Consent Statement: Written informed consent was obtained from all participants prior to inclusion. From patients below the age of 16, additional consent was acquired from their parent(s) or legal guardian.

Address reprint requests to Erik R. de Loos, MD, Department of Surgery, Division of General Thoracic Surgery, Zuyderland Medical Center, Henri Dunantstraat 5, 6419PC, Heerlen, The Netherlands. E-mails: j.daemen@zuyderland.nl e.delooos@zuyderland.nl

Keywords: Pectus excavatum, Aesthetic prediction, 3-dimensional optical surface imaging, Gaussian function

Perspective Statement

Prediction of aesthetic outcome of the Nuss procedure potentially improves preoperative information and expectation management among patients with pectus excavatum. A prediction model may objectively visualize expected postsurgical under- and overcorrection, parasternal protrusions and other asymmetries. With further development prediction of long-term postoperative aesthetic changes may be achieved.

INTRODUCTION

Pectus excavatum is an abnormal formation of the thoracic cage, characterized by an inward depression of the sternum and adjacent costal cartilage.¹⁻³ The majority of patients (ie, 80%) suffer from psychosocial complaints due to the anomalous appearance of their chest.⁴ Usually, school-aged children develop these concerns since classmates recognize and point out their disfigurement. As a consequence, patients avoid activities, such as swimming, that involve chest exposure and disengage themselves from social activities and sports.⁵⁻⁹

The Nuss procedure has been shown to be a safe surgical approach for repair of pectus excavatum, providing satisfactory aesthetic and functional outcomes that result in enhanced quality of life.^{6,10,11} Prior to correction, surgeons routinely inform patients about the expected aesthetic outcome, but this information is limited to a verbal or schematic impression. The ability to offer a sufficient visual prediction of the cosmetic result is still lacking.

Previous efforts to predict aesthetic outcome were based on a dynamic model through a mass-spring system¹² and artificial neural networks,¹³ but outcomes in these studies were limited by relative poor performance and small sample size. In this study, a different approach is proposed. The change in chest shape resulting from surgical correction may be considered as a 2-dimensional (2D) Gaussian, where the maximum coincides with the point of largest depression. Since pectus excavatum morphology is patient-specific, the 2D Gaussian should conform to patient-specific characteristics. This can be achieved by incorporating quantified morphological features of pectus excavatum based on 3-dimensional (3D) surface images, as described previously.¹⁴ Subsequently, personalized prediction models based on 2D Gaussian functions can be created. The objective of this study is to develop and evaluate a 2D Gaussian model that is personalized by patient-specific morphologic features of pectus excavatum, as a non-invasive approach to predict aesthetic outcome after the Nuss procedure.

METHODS

Study Design and Patients

A prospective, single-center cohort pilot study was conducted at Zuyderland Medical Center (Heerlen, the Netherlands). All patients who received primary surgical repair of pectus excavatum through the Nuss procedure at our clinic between May 2020 and December 2020 were requested to participate in this study. Written informed consent was obtained from all participants prior to inclusion. In case of patients below the age of 16, additional consent was acquired from their parent(s) or legal guardian. The study was approved by the

local research and ethics committee (METCZ; ID: 20200071; approval date: April 14th, 2020).

Prospective Imaging and 3D Surface Analysis

Patients received two 3D images of their anterior chest during the Nuss procedure using a handheld Artec Leo 3D imaging system (Artec3D, Luxembourg, Luxembourg). The first image was captured prior to skin incision, the second directly after Nuss bar placement. All patients were in supine position with both arms raised in front of their head. Patient position remained unaltered between images. Images were obtained within 10 seconds of controlled patient apnea to minimize motion artifacts, while surgical lights were dimmed for proper texturing. To facilitate image registration, auxiliary stripes were drawn along the four sides of the surgical drapes using a sterile marker (Fig. 1A).

Postprocessing and registration of images was performed using Artec Studio 14 (Artec3D, Luxembourg, Luxembourg). It was assumed that the bilateral, cranial and caudal sides of the chest are the least affected areas after repair. Therefore, registration was performed based on manually selected points indicated by the auxiliary stripes on the bilateral, cranial and caudal sides of the chest (Fig. 1). Finally, images were manually aligned such that the lateral axis corresponds to the system's *x*-axis, the longitudinal body axis to the *y*-axis and the antero-posterior axis to the *z*-axis.

Following image acquisition and processing, all preoperative images were subjected to the previously developed surface analysis tool.¹⁴ The tool was used to calculate the pectus depth, width, length, position and steepness from each preoperative 3D image. An additional feature was calculated to determine the rotational component, defined as the angle (θ) between the line from the deepest pectus point to the cranial border of the pectus and the line from the pectus point to the most depressed surface point at the level of the cranial border (Fig. 2). The angle was defined positive in clockwise direction.

Model Design

It was hypothesized that the deformation of the chest wall after Nuss surgery (i.e., the difference between pre- and post-operative images) may be modelled as a 2D Gaussian function. The shape of this function is generally governed by the amplitude, variance, skewness and kurtosis, while a position and

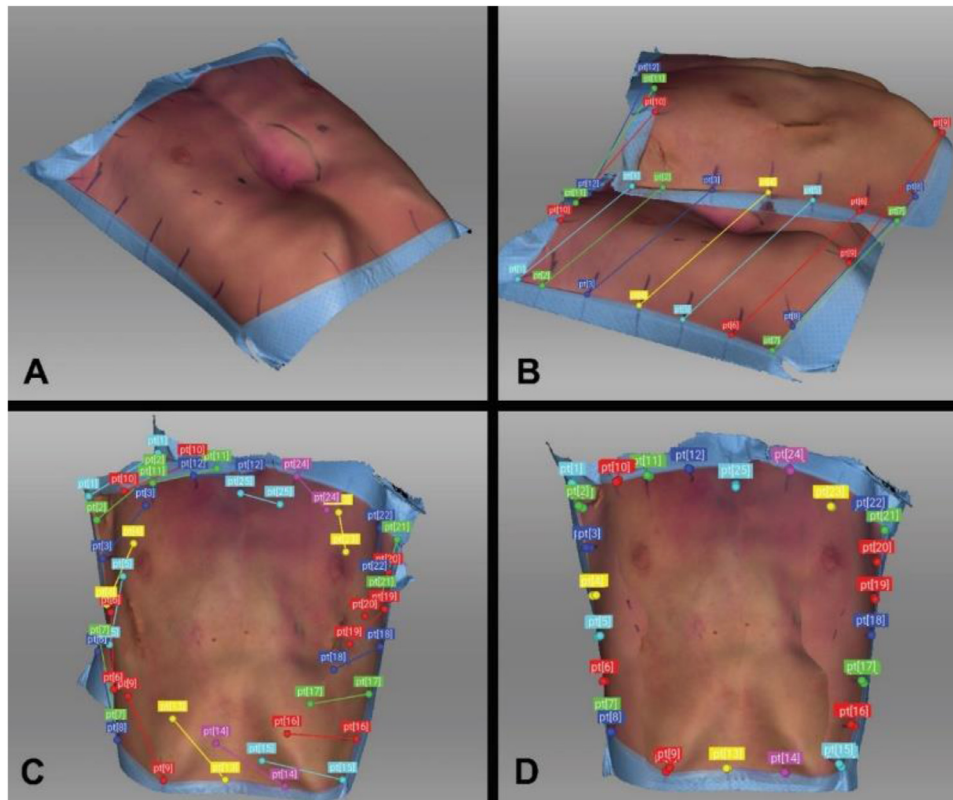


Figure 1. Registration process of pre- and postoperative 3-dimensional images. (A) Auxiliary stripes along the 4 sides of the surgical drapes. (B–C) Registration based on selected points. (D) Registered images. (Color version of figure is available online.)

rotational component contribute to the orientation of the function. This concept was used to create a patient-conformable prediction model. Morphologic features of pectus excavatum were utilized as input parameters to construct patient-specific 2D Gaussian functions. To retain versatility and allow for converging of the model, morphologic features were scaled by factors that are estimated through regression of data-fitted factors. An overview of the process is provided in Figure 3.

Amplitude, Position, and Variance

A Gaussian in the 2-dimensional space can be described as the product of two 1-dimensional Gaussian functions¹⁵:

$$f(x, y | A, \mu_x, \mu_y, \sigma_x, \sigma_y) = A \exp\left\{-\frac{(x - \mu_x)^2}{2\sigma_x^2}\right\} \exp\left\{-\frac{(y - \mu_y)^2}{2\sigma_y^2}\right\} \quad (1)$$

Here, coefficient *A* is the amplitude, μ_x, μ_y are the coordinates of the center of the peak (i.e., mean) and σ_x^2 and σ_y^2 are the variances that control the spreads of the distribution. To account for patient-specific morphological characteristics, the amplitude *A*, center μ_x, μ_y and spreads σ_x and σ_y were based on the calculated pectus depth *d*, position of deepest pectus point (*x*- and *y*-coordinates), width *w* and length *l*, respectively.

Rotation

Although the Gaussian in Equation 1 is customized using patient-specific features, it does not consider asymmetry that may be present in pectus excavatum. Asymmetry of pectus excavatum can be expressed in various forms. For instance, trench-like (long, furrow-shaped) pectus excavatum may contain a rotational component such that the longitudinal direction of the depression is not parallel to the longitudinal body axis. To account for this specific asymmetric shape, a rotational component (based on the angle of rotation θ) was incorporated in the 2D Gaussian model (see Equation 2).

Kurtosis

The shape of a function is also described by kurtosis, which is a measure of heaviness of the tails of the distribution. Platykurtic distributions have shorter tails and are flat-topped compared to normal (mesokurtic) distributions, whereas leptokurtic distributions are more sharply peaked with long tails.¹⁶ This concept can be used to incorporate the “flatness” of pectus excavatum in the prediction model. Classic cup-shaped and trench-like deformities may resemble mesokurtic to leptokurtic distributions, while a saucer-shaped pectus is more similar to a flatter platykurtic distribution. The formulation of a Gaussian function with variable tails can be taken by raising the content

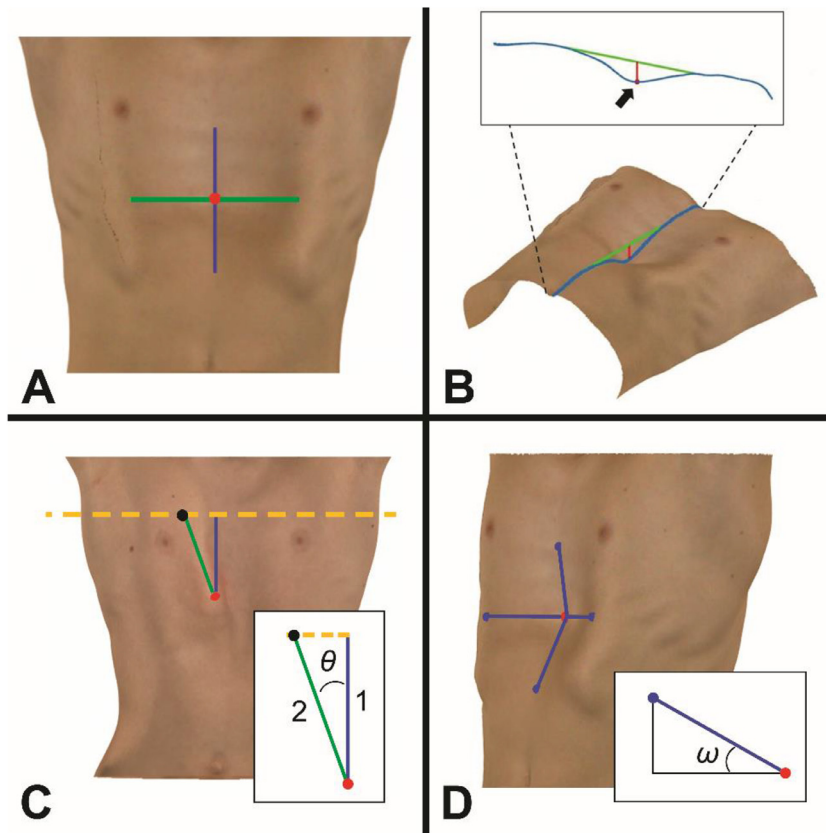


Figure 2. Patient-specific morphologic pectus features. (A) Pectus width (green), length (blue), and position (red dot). (B) Pectus depth (red line). (C) Rotational component θ , defined as the angle between (1) the line from the deepest pectus point (red dot) to the cranial border of the pectus (orange dotted line) and (2) the line from the pectus point to the most depressed surface point at the level of the cranial border (black dot). (D) Pectus steepness ω in 4 directions. (Color version of figure is available online.)

of the exponent to a power P .^{17,18} In a 2-dimensional formulation, the function can be combined with potentially different powers P_x and P_y , see Equation 2.

Skewness

Asymmetry of pectus excavatum may also be expressed as the inequality of the opposing pectus steepness angles, both in lateral and longitudinal direction. To reflect this form of asymmetry, a skewness component was implemented. A multivariate skew-normal distribution can be realized by the multiplication of the normal probability density function ϕ and the normal cumulative distribution function Φ .^{19,20} In this study a similar approach was applied by multiplying the 2-dimensional Gaussian function with 2 subsequent normal cumulative distribution functions to produce independent skewness components in two dimensions (see Equation 2). The cumulative distribution functions were obtained from the normalized 1-dimensional Gaussian function excluding rotation and kurtosis components. The skewness parameters α_x and α_y determine the slope of the cumulative distribution functions and are estimated using the transversal pectus steepness ω_t and the

longitudinal pectus steepness ω_l , respectively. The transversal pectus steepness is defined as the difference in bilateral pectus steepness ($\omega_t = \omega_{right} - \omega_{left}$), whereas the longitudinal pectus steepness is the difference in caudal and cranial steepness ($\omega_l = \omega_{caudal} - \omega_{cranial}$).

The differences were defined such that a positive α_x leads to a left-skewed distribution whereas a positive α_y results in cranial skewness. For example, the correction of an asymmetric pectus excavatum with a larger right steepness angle ($\omega_{right} > \omega_{left}$) requires a steeper distribution function on the right side than the left. Therefore, in this case, the correction should follow a left-skewed distribution. The introduction of skewness shifts the distribution peak from its original position. Therefore, the distribution was repositioned to ensure that its peak is aligned with the point of largest depression in the chest.

Model Formulation

All previously stated components were combined into a single model. As such, this model adapts to various specific morphologic characteristics of pectus excavatum. The model formulation is:

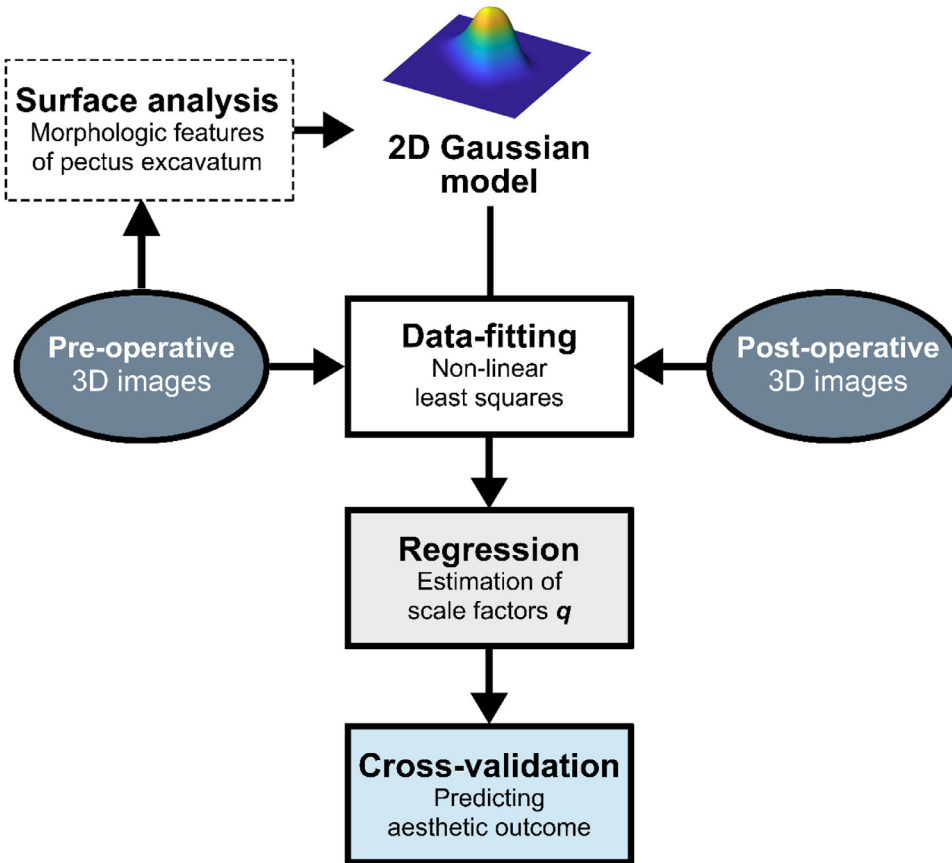


Figure 3. Development and validation process of a 2-dimensional (2D) Gaussian model to predict aesthetic outcome after Nuss procedure.

$$f(x, y | A, \mu_x, \mu_y, \sigma_x, \sigma_y, P_x, P_y) = 4\phi\Phi_x\Phi_y$$

with $\phi = A \exp\left\{-\left(\frac{h_x^2}{2\sigma_x^2}\right)^{P_x}\right\} \exp\left\{-\left(\frac{h_y^2}{2\sigma_y^2}\right)^{P_y}\right\}$

and $h_x = (x - \mu_x) \cos\theta - (y - \mu_y) \sin\theta$

$$h_y = (x - \mu_x) \sin\theta + (y - \mu_y) \cos\theta \quad (2)$$

where θ is the angle of rotation and P_x and P_y the kurtosis components. The normal cumulative distribution functions Φ_x and Φ_y are given by:

$$\Phi(u) = \frac{1}{2} \left[1 + \operatorname{erf}\left(\frac{u}{\sqrt{2}}\right) \right]$$

with $u_x = \alpha_x \frac{x - \mu_x}{\sigma_x}$ $u_y = \alpha_y \frac{y - \mu_y}{\sigma_y}$ (3)

and $\operatorname{erf}\left(\frac{u}{\sqrt{2}}\right) = \frac{2}{\sqrt{\pi}} \int_0^{\frac{u}{\sqrt{2}}} e^{-t^2} dt$

and where α_x and α_y are the skewness parameters. The size of the Gaussian function is equal to the dimensions of the region of interest of the chest, that is, pectus area.¹⁴

Nonlinear Least-squares Data-fitting

Although the shape components generate patient-specific distribution functions, the model may be improved by implementing posterior knowledge acquired from the postoperative 3D images. For this purpose, a prediction vector \mathbf{q} with factors $q_A, q_{\sigma_x}, q_{\sigma_y}, q_{\alpha_x}, q_{\alpha_y}, q_{P_x}, q_{P_y}$ was used to scale the corresponding input features. Note that the rotation angle θ and the position (μ_x, μ_y) were directly applied without scaling. The remaining components are defined in Table 1.

Table 1. Definitions of the Model Input Parameters

Model Input Parameter	Definition
Amplitude	$A = q_A d$
Spread (transverse)	$\sigma_1 = q_{\sigma 1} w$
Spread (longitudinal)	$\sigma_2 = q_{\sigma 2} l$
Skewness (transverse)	$\alpha_1 = q_{\alpha 1} \frac{\omega_t}{ \omega_l }$
Skewness (longitudinal)	$\alpha_2 = q_{\alpha 2} \frac{\omega_l}{ \omega_t }$
Kurtosis (transverse)	$P_1 = q_{P 1}$
Kurtosis (longitudinal)	$P_2 = q_{P 2}$

Morphologic features of pectus excavatum (d = pectus depth, w = pectus width, l = pectus length, ω_t = transversal pectus steepness and ω_l = longitudinal pectus steepness) are scaled by the corresponding prediction scale factor q .

Consider the matrices \mathbf{J} and \mathbf{Z} as the 3D surface heights of the anterior chest wall prior to and directly after surgery, respectively. The prediction of \mathbf{Z} is the estimation:

$$\hat{\mathbf{Z}} = \mathbf{J} + f(\mathbf{x} | \mathbf{q}) \tag{4}$$

where f is the distribution of the model and $\mathbf{x} = (x, y)$. It is desired to find the prediction scales \mathbf{q} such that the predicted outcome $\hat{\mathbf{Z}}$ best fits the given postoperative data \mathbf{Z} , by minimizing the sum of the squared residuals S . This can be described as a nonlinear least-squares problem²¹:

$$\begin{aligned} \text{minimize } S(\mathbf{q}) &= \sum_{i=1}^k \mathbf{Z} - \hat{\mathbf{Z}}^2 \\ &= \sum_{i=1}^k \mathbf{Z} - (\mathbf{J} + f(\mathbf{x} | \mathbf{q}))^2 \end{aligned} \tag{5}$$

where k is the number of elements in \mathbf{Z} . The prediction scales \mathbf{q} were calculated per model and for each patient separately. The lower bounds were set to zero to inhibit negative solutions: $\mathbf{q} = [0, \infty)$. The starting points of the minimization function were chosen such that the distribution is mesokurtic ($q_{px}, q_{py} = 1$), but slightly skewed ($q_{\alpha x}, q_{\alpha y} = 1$) and that its height, and transversal and longitudinal standard deviations equals the pectus depth, width and length, respectively ($q_A, q_{\sigma x}, q_{\sigma y} = 1$).

Evaluation of Data-fitted Models

By minimizing S , values for \mathbf{q} are estimated such that the prediction best fits the target outcome. For each patient, the aesthetic outcome after data-fitting was estimated using the patient-specific \mathbf{q} scale factors. To evaluate the performance of the model at this stage, all outcomes were compared to the postoperative images by calculating the root mean squared deviation and the maximum negative and positive differences.

The effect of the model attenuates at the peripheral surfaces of the chest. If these areas were to be included in the calculation of the root mean squared deviation, they could outweigh the deviations occurring in the pectus area, where the model’s effect is greatest. Therefore, the calculations were performed within a delimited area, the pectus area. The pectus area is defined as a rectangular area that is cranially, caudally and bilaterally bordered by the most anterior surface points in the corresponding direction.¹⁴

Regression and Cross-validation

To estimate the prediction scale factors without posterior knowledge of postoperative images, regression models were established. An exponential regression model was produced to estimate the scale factor q_A , whereas linear regression models were used to estimate $q_{\sigma 1}, q_{\sigma 2}, q_{\alpha 1}, q_{\alpha 2}, q_{p1}$ and q_{p2} . For each regression model, the goodness of fit was evaluated through the R^2 value.

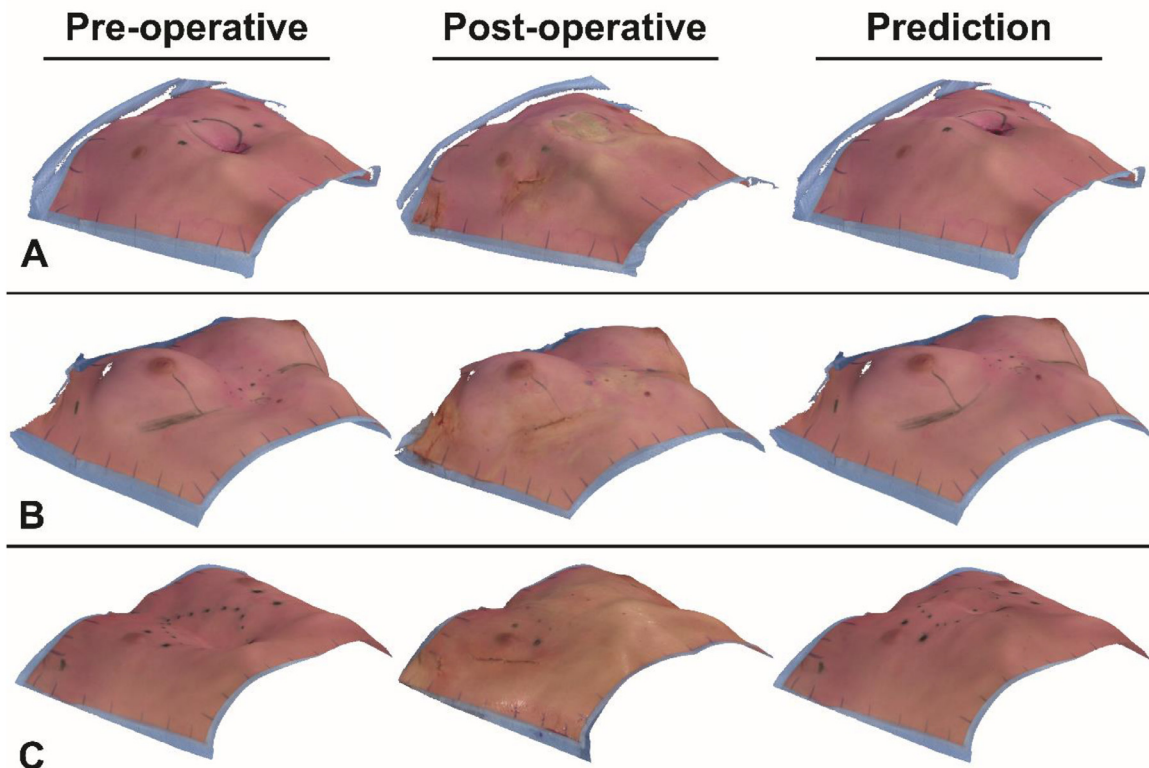


Figure 4. Examples of predicted aesthetic outcome in patients with pectus excavatum. (A) Patient 7, (B) patient 8, (C) patient 28. From left to right: preoperative, postoperative, and prediction images. The predicted reconstruction utilizes the preoperative image texture to retain the patient’s appearance.

Leave-one-out cross-validation was carried out to estimate the performance of the prediction model based on the regression models. The root mean squared deviation and maximum positive and negative deviations in the pectus area were used as measures of performance. The overall performance of the model was reported as mean and standard deviation of the performances achieved in each iteration of the cross-validation.

RESULTS

Thirty consecutive patients underwent surgical correction of pectus excavatum by the Nuss procedure and received 3D imaging of their chest during the procedure. The median age was 15.5 years (interquartile range [IQR]: 14.5–17.4) and 90% were males. Examples of pre- and postoperative images and predicted aesthetic outcomes are shown in Figure 4.

The performance of the prediction model is indicated by the root mean squared deviations and the maximum negative and positive differences between prediction and postoperative outcome (see Table 2). The average of the root mean squared deviations obtained through data-fitting was 4.4 ± 2.1 mm. Following cross-validation of the actual prediction model, the average of the root mean squared deviations was 6.3 ± 2.0 mm. All deviations after data-fitting and during cross-validation are provided in Supplementary Material Table 1 and Supplementary Material Table 2, respectively.

In Table 3, the averages and standard deviations of the R^2 values of the regression models are presented. The regression model to estimate the scale factor for the amplitude achieved the highest score ($41\% \pm 2\%$), while in 3 out of 7 regression models the average R^2 value was smaller than 5%.

Figure 5 shows the predicted outcome of each validation sample in the cross-validation, with a colored overlay that corresponds to the difference between the predicted and the postoperative images. Key outcomes are summarized in Figure 6.

DISCUSSION

This study developed and evaluated a noninvasive method to predict aesthetic outcome after the Nuss procedure based on 3D images of patients with pectus excavatum. Up until now, no prediction tool exists that can be clinically used to offer patients with pectus excavatum a visual impression of the

Table 3. Mean R-square Values for the Cross-validated Regression Model

Regression Model	R^2 (Mean \pm SD [%])
\hat{q}_A	41 ± 2
$\hat{q}_{\sigma 1}$	18 ± 2
$\hat{q}_{\sigma 2}$	0 ± 1
$\hat{q}_{\alpha 1}$	27 ± 2
$\hat{q}_{\alpha 2}$	32 ± 3
$\hat{q}_{p 1}$	5 ± 1
$\hat{q}_{p 2}$	4 ± 2

SD = standard deviation.

appearance of their chest after surgery. Simulation of the aesthetic results may help patients and surgeons understand how a procedure changes the physical aspect of a patient, with the aim to improve expectation management and reduce perioperative stress. Even after surgical repair of pectus excavatum, the chest may still exhibit anomalies compared to a non-diseased chest wall. A plain statement that the patient’s chest will resemble a normal chest would therefore not suffice, whereas a prediction tool would demonstrate and visualize more adequate outcomes.

As an example, the pectus deformity in patient 7 was preoperatively asymmetric due to protruding parasternal cartilage on the right side. The prediction model emphasized this asymmetry by a slight overcorrection in this area (Figs. 4A and 5; patient 7.). During visual comparison of the prediction with the postoperative image by a thoracic surgeon, the outcome was considered similar since the protrusion remained in the actual postoperative outcome. In clinical practice, this might be a case wherein the prediction tool can be used to inform patients about postoperative persisting irregularities.

The results show that data-fitted reconstructions of the chest wall have relatively low root mean squared deviations (4.4 ± 2.1 mm). However, in one patient (#15) the root mean squared deviation after data-fitting was noticeably larger (10.8 mm), see Supplementary Material Table 1. When evaluating morphologic features,¹⁴ patient 15 contained a remarkably deep deformity (42 mm) in combination with significant asymmetry (–16%) compared to other study subjects (median and IQR pectus depth: 17 (33) mm; median and IQR asymmetry: –1% (6.5%), $N = 29$). Considering these results, it might be beneficial to distinguish patients with eccentric pectus excavatum. Models specifically developed for such subgroups could increase overall prediction performances. Patients can be classified based on the degree of 3-dimensional surface features, such as the pectus depth or degree of asymmetry, or combinations of features. However, to determine whether classification is feasible and developing type-specific prediction models increases performance, study population size should be increased. A rule of thumb to estimate the required sample size is to use the ratio of events per variable, where a ratio of 10:1 is considered the minimum for a model to make valid predictions.²² Thus, for a model with seven variables, at least 70

Table 2. Performance Measures After Data-Fitting and After Regression

		Mean \pm SD (mm)
Performance of data-fitted prediction model	Root mean squared deviation	4.4 ± 2.1
	Maximum negative deviation	-11.7 ± 5.3
	Maximum positive deviation	9.2 ± 6.1
Performance of prediction with regression model	Root mean squared deviation	6.3 ± 2.0
	Maximum negative deviation	-10.2 ± 5.7
	Maximum positive deviation	12.7 ± 6.1

SD = standard deviation.

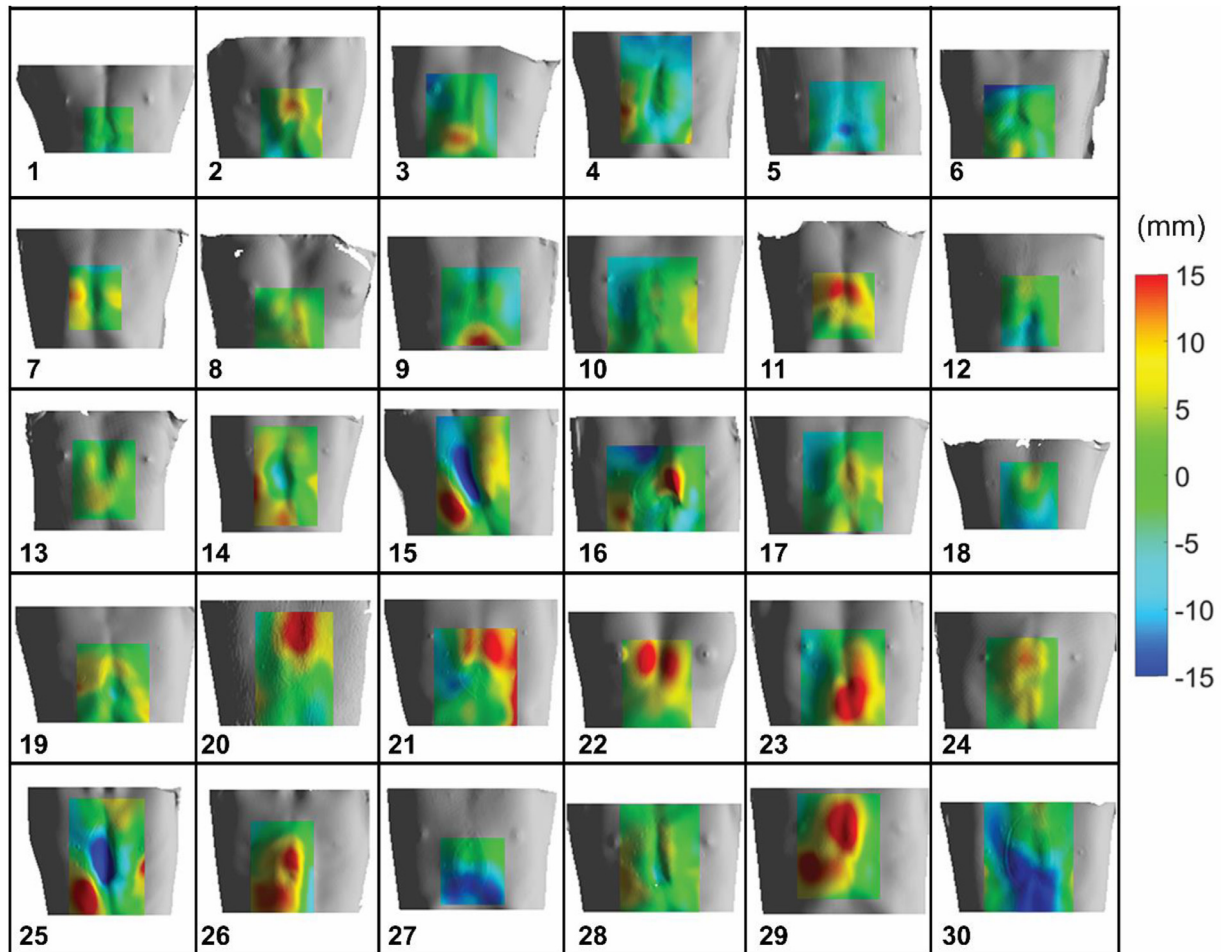


Figure 5. Predicted aesthetic outcomes in patients with pectus excavatum. Predictions are overlaid with a color-coded map corresponding to the difference with the postoperative images. Scales are in millimeters.

patients are required per type-specific subgroup. Especially for less frequent types this may be difficult to achieve.

Limitations

The prediction of aesthetic outcome and calculation of performance measures were restricted to the pectus area. However, the bar may press the supporting ribs inward, thereby altering the bilateral chest wall. A prediction including the bilateral chest wall may provide a more comprehensive representation of the expected outcome. To accommodate this, the model may be extended with negative Gaussians or similar functions that simulate the depression of the ribs.

Developing a valid prediction tool relies on proper alignment and registration of pre- and postoperative images. Registration and alignment processes were not quantitatively evaluated, potentially introducing deviations and bias. For instance, registration was based on the assumption that the sides of the chest are less affected than the center area after repair. However, aesthetic changes outside the pectus area may still occur, such as a depression of the ribs that support the pectus bar. Additionally, one should consider that the

reproducibility of 0.48 mm²³ of the imaging device may cause inevitable, yet slight deviations. Further research should include an evaluation on registration accuracy and clarify to what extent registration deviations and the reproducibility of the imaging device affect prediction.

The prediction performance of the model is also limited by the capability of the regression methods used to estimate the scale factors. As presented in Table 2, prediction deviations increased after regression compared to the outcomes after data-fitting. Particularly in patient 29, the root mean squared deviation of the prediction was 9.5 mm (see Supplementary Material Table 2), whereas in the data-fitted reconstruction this deviation was only 3.8 mm (see Supplementary Material Table 1). This suggests that presence of noise in the data results in inadequate regressions, limiting the prediction capacity of the model.

Noise may be a consequence of several events. For instance, the minimization problem stated in Equation 5 may have multiple satisfactory solutions with varying combinations of scale factors. Although 1 combination may result in a minimized deviation on individual basis, another combination might be

Prediction of aesthetic outcome in pectus excavatum

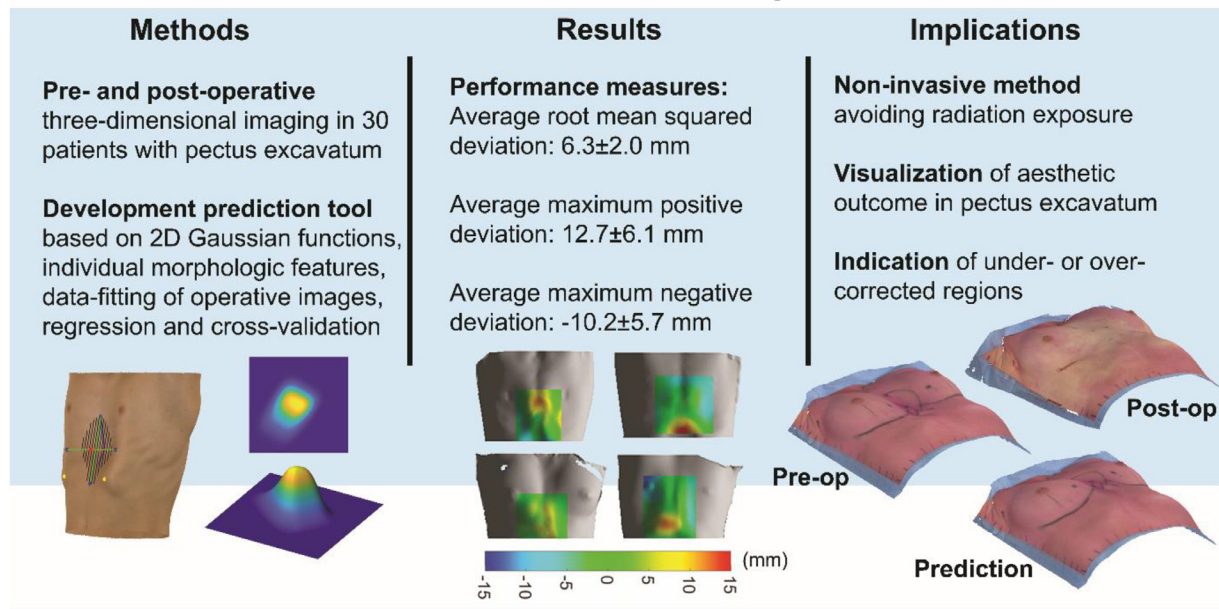


Figure 6. An automatic prediction tool was developed to visualize aesthetic outcome of pectus excavatum based on 3-dimensional images. Clinical implications include noninvasive and objective visualization of aesthetic outcome, that may indicate postsurgical under- or overcorrection. (Pre-op = preoperative, Post-op = postoperative.)

more beneficial in a global perspective to increase predictability. Related to this, the minimization function might terminate in a local minimum, unable to find other minima that are more appropriate. The selected starting values are therefore crucial in the search for a minimum. Here, starting points were chosen such that the distribution is mesokurtic, but slightly skewed and that its height, and transversal and longitudinal standard deviations equals the pectus depth, width and length, respectively. Any other combination of starting points may result in different outcomes.

Another cause of noise in the data is the dependency of selected scale factors on postsurgical outcomes. The Nuss procedure involves the implementation of a personalized bar, of which the size, shape and position are determined during surgery. Therefore, outcomes rely on the surgeon's judgement and skill, possibly introducing variability in the target data. Including the bar shape and other surgical parameters in the model may increase performance, but requires substantial preoperative planning at an early stage in the clinical workup. Further research should evaluate the potential benefits of including the bar shape in the prediction model at the cost of a more complex model.

Implications

Three-dimensional imaging has been introduced in the clinical workup of pectus excavatum as a noninvasive alternative to conventional imaging modalities which require ionizing radiation. Previous studies have shown that optically derived severity indices (e.g., the equivalent Haller index) may be used as

alternative measures to quantify severity of pectus excavatum²⁴ and that morphologic features of the deformity can be derived automatically from 3D images.¹⁴ New technologies being introduced in healthcare should improve patient care while reducing costs. Multifunctional technology based on automatic processes can increase its value and avoid costly and labor-intensive procedures. In addition to patient-safety, diagnostics and documentation, 3D optical imaging may improve patient care of pectus excavatum through enhanced communication and consensus, surgical decision-making and patient follow-up.

Future Perspectives

This study presents a method for predicting aesthetic outcome in patients with pectus excavatum, but additional steps should be undertaken to make this a functional tool. Since this tool is intended as a consultation aid in the clinical setting, predictions should be obtained in the preoperative phase. Thus, the next step is to develop a model using full circumferential 3D images of the patient's torso in upright position that are obtained in the diagnostic process and according to our previously developed imaging protocol.²⁵ In this way, images are more representative to the patient's natural pose while ensuring homogeneity between images regarding the respiration cycle. In addition, these images yield more valuable information, such as the cross-sectional diameters required for automatic axis alignment and can facilitate development of a prediction model that includes the bilateral chest wall. Re-evaluation of

prediction accuracy should be performed for subsequent models that are designed to use in clinical practice.

At this stage, the predictions are a representation of the chest directly after surgery, but do not consider aesthetic variances over time. For instance, a costal cartilage ring may be highlighted directly after surgery, but may gradually diminish due to remodeling of the ribs and cartilage. Other long-term variances may be caused by for instance thoracic muscle growth and body mass index. In addition, relapse of overcorrected regions or a recurrence of pectus excavatum with varying degrees of chest wall depression may occur after bar removal.^{26,27} Thus, this study describes a method to predict post-operative chest aesthetics, but with further developments the model may be extended to generate long-term predictions. Nonetheless, chest wall appearance directly after surgery reflects what the patient may expect after waking up from anesthesia. Ultimately, predictions that visualize the chest at different stages, thereby showing anatomical changes over time, may enhance comprehension and manage expectations of patients during consultation.

Finally, to implement a technology in clinical practice, both validation and justification should be investigated. Currently neither a quantitative nor a qualitative gold-standard to which a prediction model should comply for clinical feasibility has been established. A clinically acceptable error rate may be determined based on judgment and satisfaction of patients and surgeons, which should be a subject of future research. Concurrent to this, the clinical value of both short- and long-term predictions should be investigated by evaluation of patient satisfaction and reduction in perioperative stress. Furthermore, applicability of the prediction model to slight differences in standardized techniques of the Nuss procedure should be evaluated. A subsequent cost analysis should be performed to justify the implementation of 3D imaging technology in patient care of pectus excavatum.

CONCLUSION

A two-dimensional Gaussian model based on 3D optical surface images is a clinically promising tool to predict post-operative aesthetic outcome in patients suffering from pectus excavatum. Further research should focus on additional steps to decrease maximum deviations (e.g., by increasing sample size and assessing subtype-specific models), include long-term predictions, assess related health benefits and facilitate clinical implementation of this tool.

AUTHORS' CONTRIBUTIONS

NC: conceptualization, methodology, image acquisition, data processing, software, formal analysis, visualization, writing — original draft. JD: conceptualization, methodology, funding acquisition, writing — review and editing. CS: conceptualization, methodology, supervision, writing — review and editing. NJ: writing — review and editing. YJ: writing — review and editing. JM: supervision, writing — review and editing. YV:

conceptualization, methodology, supervision, writing — review and editing. KH: conceptualization, supervision, writing — review and editing. EdL: conceptualization, methodology, supervision, writing — review and editing.

SUPPLEMENTARY MATERIAL

Scanning this QR code will take you to the article title page to access supplementary material.



REFERENCES

1. Chung CS, Myriantopoulos NC: Factors affecting risks of congenital malformations. I. Analysis of epidemiologic factors in congenital malformations. Report from the collaborative perinatal project. *Birth Defects Orig Artic Ser* 11:1–22, 1975
2. Krasopoulos G, Dusmet M, Ladas G, et al: Nuss procedure improves the quality of life in young male adults with pectus excavatum deformity. *Eur J Cardiothorac Surg* 29:1–5, 2006
3. Cobben JM, Oostra R-J, van Dijk FS: Pectus excavatum and carinatum. *Eur J Med Genet* 57:414–417, 2014
4. Habelt S, Korn S, Berger A, et al: Psychological distress in patients with pectus excavatum as an indication for therapy. *Int J Clin Exp Med* 2:295, 2011
5. Kelly RE, Nuss D: Pectus excavatum. *Pediatric Thoracic Surgery*. London, Springer; 2009, pp 535–545
6. Kelly RE, Cash TF, Shamberger RC, et al: Surgical repair of pectus excavatum markedly improves body image and perceived ability for physical activity: multicenter study. *Pediatrics* 122:1218–1222, 2008
7. Williams A, Crabbe D: Pectus deformities of the anterior chest wall. *Paediatr Respir Rev* 4:237–242, 2003
8. Steinmann C, Krille S, Mueller A, et al: Pectus excavatum and pectus carinatum patients suffer from lower quality of life and impaired body image: a control group comparison of psychological characteristics prior to surgical correction. *Eur J Cardiothorac Surg* 40:1138–1145, 2011
9. Ji Y, Liu W, Chen S, et al: Assessment of psychosocial functioning and its risk factors in children with pectus excavatum. *Health Qual Life Outcomes* 9:28, 2011
10. Croitoru DP, Kelly RE Jr, Goretsky MJ, et al: Experience and modification update for the minimally invasive Nuss technique for pectus excavatum repair in 303 patients. *J Pediatr Surg* 37:437–445, 2002
11. Casamassima MGS, Gause C, Goldstein SD, et al: Patient satisfaction after minimally invasive repair of pectus excavatum in adults: Long-term results of nuss procedure in adults. *Ann Thorac Cardiovasc Surg* 101:1338–1345, 2016
12. Moreira AH, Rodrigues PL, Fonseca J, et al: Pectus excavatum postsurgical outcome based on preoperative soft body dynamics simulation. *Med Imaging* 2012 8316:83160K, 2012
13. Vilaça JL, Moreira AH, Pedro L, et al: Virtual simulation of the postsurgical cosmetic outcome in patients with pectus excavatum. *Med Imaging* 2011 7964:79642L, 2011
14. Coorens NA, Daemen JHT, Slump CH, et al: The automatic quantification of morphological features of pectus excavatum based on three-dimensional images. *Semin Thorac Cardiovasc Surg* 2012
15. Bachor H-A, Ralph TC, Lucia S, et al: *A Guide to Experiments in Quantum Optics*. Weinheim, Wiley-VCH; 2004

16. Balanda KP, MacGillivray H: Kurtosis: a critical review. *Am Stat* 42:111–119, 1988
17. Gori F: Flattened gaussian beams. *Opt Commun* 107:335–341, 1994
18. Parent A, Morin M, Lavigne P: Propagation of super-gaussian field distributions. *Opt Quantum Electron* 24:S1071–S1079, 1992
19. Azzalini A, Valle AD: The multivariate skew-normal distribution. *Biometrika* 83:715–726, 1996
20. Tian W, Wang C, Wu M, et al: The multivariate extended skew normal distribution and its quadratic forms. *Causal Inference in Econometrics*. Cham, Springer; 2016, pp 153–169
21. Griva I, Nash SG, Sofer A: *Linear and Nonlinear Optimization*. Philadelphia, Siam; 2009
22. Seel RT, Steyerberg EW, Malec JF, et al: Developing and evaluating prediction models in rehabilitation populations. *Arch Phys Med Rehabil* 93: S138–S153, 2012
23. Daemen JHT, Loonen TGJ, Verhulst AC, et al: Three-dimensional imaging of the chest wall: a comparison between three different imaging systems. *J Surg Res* 259:332–341, 2021
24. Daemen JHT, Coorens NA, Hulsewé KWE, et al: Three-dimensional surface imaging for clinical decision making in pectus excavatum. *Semin Thorac Cardiovasc Surg* 2021
25. Daemen JHT, Loonen TGJ, Coorens NA, et al: Photographic documentation and severity quantification of pectus excavatum through three-dimensional optical surface imaging. *J Vis Commun Med*: 1–8, 2020
26. Cho DG, Kim JJ, Park JK, et al: Recurrence of pectus excavatum following the nuss procedure. *J Thorac Dis* 10:6201, 2018
27. Luu TD, Kogon BE, Force SD, et al: Surgery for recurrent pectus deformities. *Ann Thorac Surg* 88:1627–1631, 2009